Current Biology

Supplemental Information

A Developmental Framework for Graft Formation and Vascular Reconnection in *Arabidopsis thaliana*

Charles W. Melnyk, Christoph Schuster, Ottoline Leyser, and Elliot M. Meyerowitz

Supplemental Data

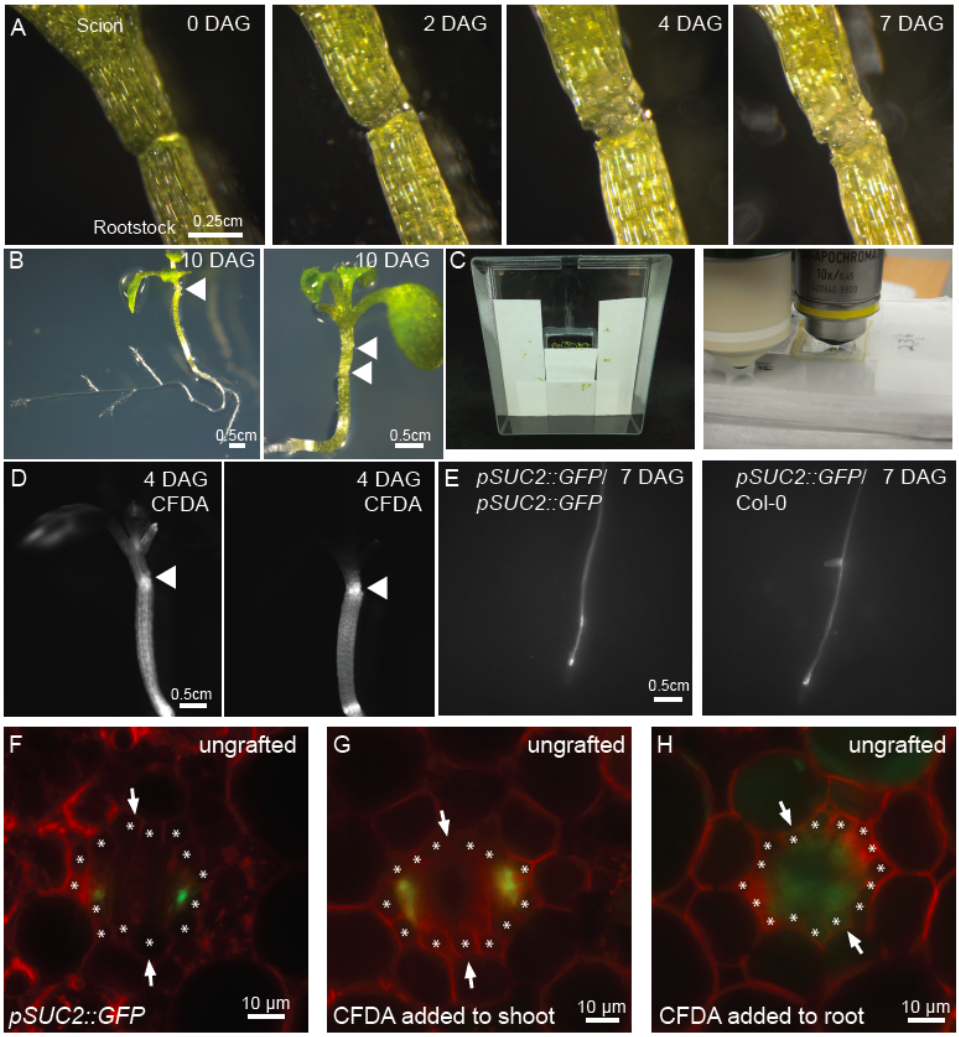

Figure S1. Techniques used to visualise graft formation and vascular reconnection, related to Figure 1.

A) A Col-0/Col-0 (scion/rootstock notation) graft junction monitored from 0 to 7 days after grafting (DAG) using brightfield optics.

B) Two (right) and three (left) segment (termed interstock) graft junctions of Col-0 plants. Triangles denote graft junctions.

C) Humidity chamber (left panel) for grafting *Arabidopsis* plants on a coverslip, which allows live imaging of graft junctions under a confocal microscope for up to 10 days (right panel).

D) Carboxyfluorescein diacetate (CFDA) added to the rootstock, and fluorescence in the leaf vasculature monitored at 4 DAG. Some plants showed transport of dye to the scions (left panel), whereas others did not (right panel). After moving through the vascular tissue, CFDA moved radially outwards into the stele, mesophyll and epidermis.

E) A *pSUC2::GFP* Col-0 scion grafted to a *pSUC2::GFP* Col-0 rootstock (left panel) or Col-0 rootstock (right panel). GFP moved across the graft junction and into the rootstock of *pSUC2::GFP*/Col-0 grafts between 3-4 DAG.

F-H) Transverse sections through an ungrafted hypocotyl showed that the *SUC2* promoter drives GFP expression in the phloem companion cells (F). When CFDA is added to the shoots, fluorescent signal is detected in the phloem of the hypocotyl (G). When CFDA is added to the roots, fluorescence is detected in the xylem and surrounding cells of the hypocotyl (H). Panel (F) is stained with FM4-64. Panels (G) and (H) are in the *pUBQ10::PM-tdTomato* background which localises red fluorescent protein to the cell membranes. Asterisks indicate pericycle cells, and arrows point to the orientation of the xylem.

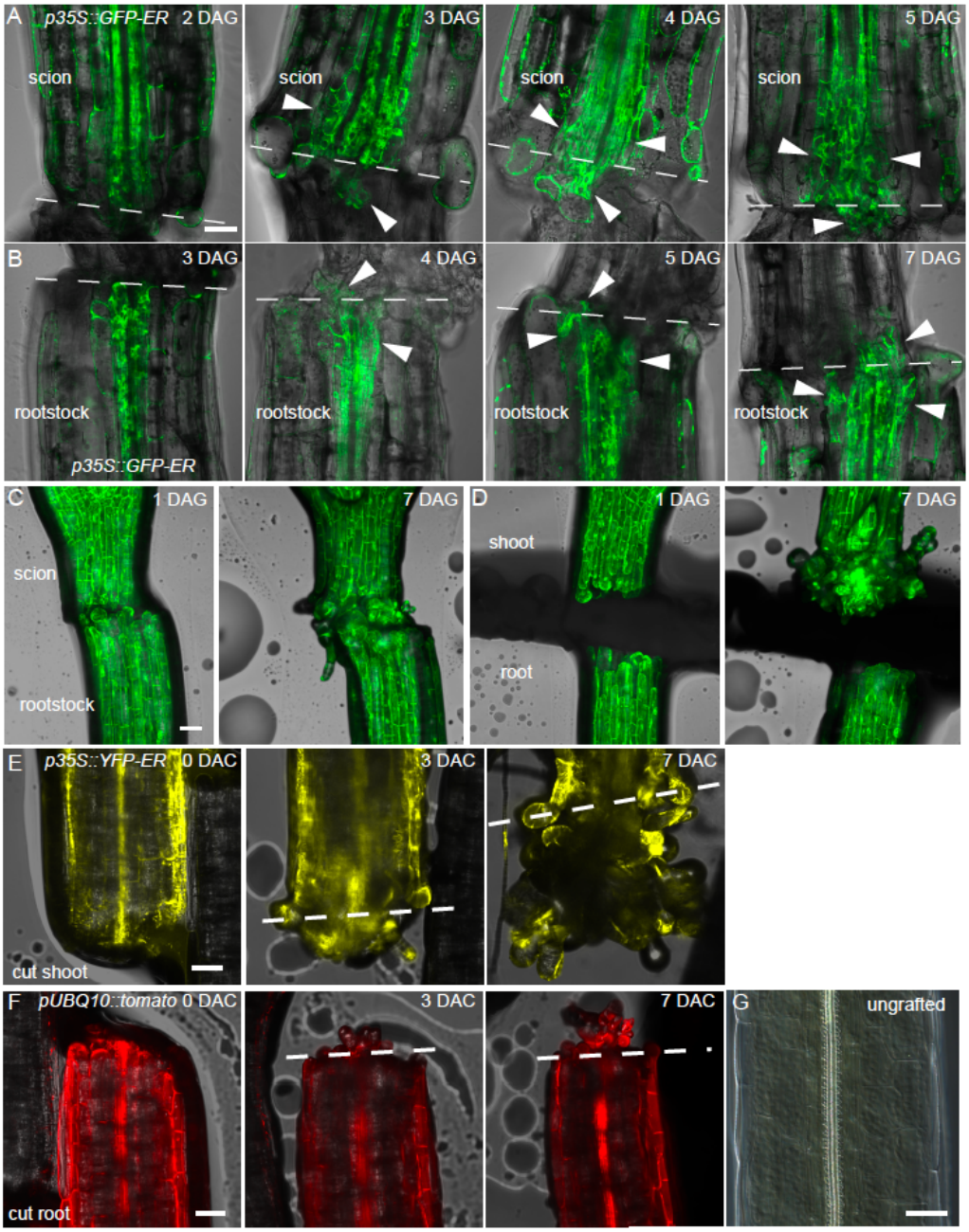

Figure S2. Cell expansion, cell proliferation and gene expression are affected upon graft formation, related to Figure 2.

A-B) Vascular cells expand and proliferate at the graft junction. Longitudinal hand sections through scions expressing *p35S::GFP-ER* show cell growth beginning 2 DAG (A), whereas rootstocks expressing *p35S::GFP-ER* show cell growth beginning 3 DAG (B). Triangles indicate expanded and growing cells.

C-D) Contact between the scion and the rootstock restricts cell division and expansion in the scion (C), whereas when the two hypocotyl halves are separated by a parafilm barrier (D), high levels of cell expansion and proliferation in the shoot occur 7 DAG in *p35S::GFP* expressing plants.

E-F) Cells expand and proliferate at the surface of a cut hypocotyl shoot half (E) between 0 to 7 days after cutting (DAC) in *p35S::YFP-ER* expressing plants. A cut hypocotyl root half (F) shows less expansion, which is localised to the centre of the hypocotyl in *pUBQ10::PM-tdTomato* expressing plants.

G) Xylem vessels (spiral structures) in a cleared whole mount ungrafted hypocotyl visualised using DIC optics.

A-G) Scale bar is 50μm. Dashed lined represents the graft or cut site.

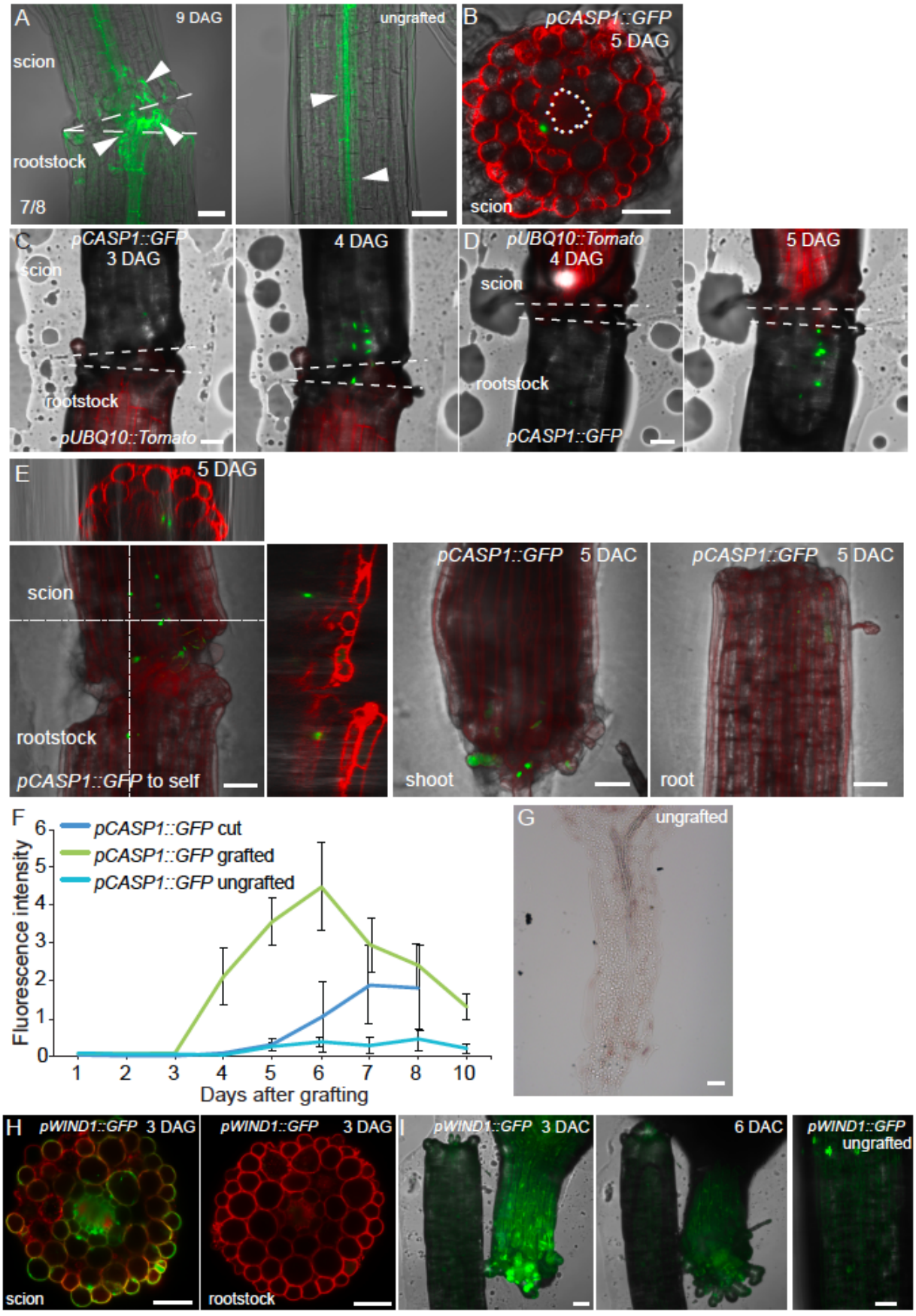
A
9 DAG
scion
rootstock
7/8
ungrafted
B
pCASP1::GFP
5 DAG
scion
C
pCASP1::GFP
3 DAG
scion
rootstock
pUBQ10::Tomato
4 DAG
D
pUBQ10::Tomato
4 DAG
scion
rootstock
pCASP1::GFP
5 DAG
E
5 DAG
scion
rootstock
pCASP1::GFP to self
pCASP1::GFP 5 DAC
shoot
pCASP1::GFP 5 DAC
root
F
pCASP1::GFP cut
pCASP1::GFP grafted
pCASP1::GFP ungrafted
Fluorescence intensity
Days after grafting
G
ungrafted
H
pWIND1::GFP 3 DAG
scion
pWIND1::GFP 3 DAG
rootstock
I
pWIND1::GFP 3 DAC
6 DAC
pWIND1::GFP
ungrafted

Figure S3. Cell proliferation dynamics at the graft junction, related to Figure 3.
A) Autofluorescence of lignin (white triangles) at the graft junction (dashed line) suggests that the Casparian strip network is reformed at 9 DAG. Bottom left number represents the number of individuals with a continuous lignin network across the graft junction at this time point.
B) In transverse hand sections 50μm above the graft junction, *pCASP1::NLS-GFP* is expressed in endodermal cells at five DAG. Asterisks represent the pericycle cells and the section is counterstained with FM4-64.
C-D) Scions (C) or rootstocks (D) expressing *pCASP1::NLS-GFP* were grafted to plants expressing *pUBQ10::PM-tdTomato*. *pCASP1* expresses earlier in scions than in rootstocks.
E) *pCASP1::NLS-GFP* is upregulated in grafted individuals (left panel), but not in cut roots (right panel) and to lower levels in cut shoots (middle panel) 5 DAG or 5 DAC. Inserts above and to the right show orthogonal views of the left panel (dotted lines). In all panels, hypocotyls are counterstained with FM4-64.
F) *pCASP1::NLS-GFP* plants were self-grafted, and mean fluorescence intensity for 13 individuals showed a peak of expression 6 DAG. Fluorescence intensity was lower in cut (n=4) and ungrafted (n=5) individuals (+/- SEM). The same plants were imaged and quantified daily, and a representative individual is shown in Figure 3C.
G) Ungrafted individuals did not show substantial *Histone H4* staining in the hypocotyl.
H) Transverse hand sections from grafted plants 50μm above (left panel) or 50μm below (right panel) the graft junction showed *pWIND1::GFP* upregulation in the hypocotyl scion, but not in the hypocotyl rootstock at 3 DAG in plants expressing *pUBQ10::PM-tdTomato*.
I) Cut hypocotyls upregulated *pWIND1::GFP* expression in the shoot, but not in the root. Ungrafted plants showed a low level of *pWIND1::GFP* expression.
A-I) Scale bar, 50μm.

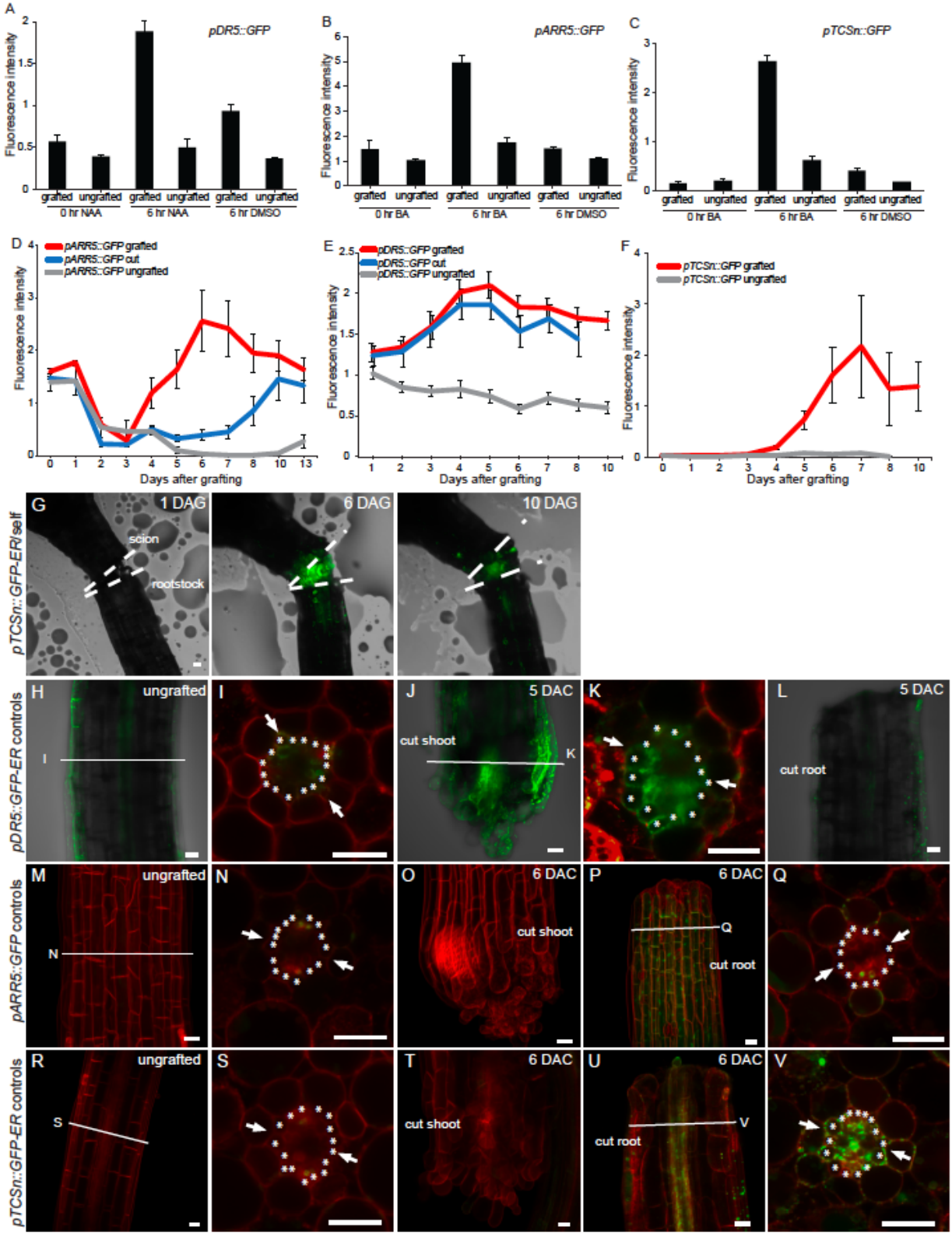
A
pDR5::GFP
Fluorescence intensity
grafted ungrafted grafted ungrafted grafted ungrafted
0 hr NAA
6 hr NAA
6 hr DMSO
B
pARR5::GFP
Fluorescence intensity
grafted ungrafted grafted ungrafted grafted ungrafted
0 hr BA
6 hr BA
6 hr DMSO
C
pTCSn::GFP
Fluorescence intensity
grafted ungrafted grafted ungrafted grafted ungrafted
0 hr BA
6 hr BA
6 hr DMSO
D
pARR5::GFP grafted
pARR5::GFP cut
pARR5::GFP ungrafted
Fluorescence intensity
Days after grafting
E
pDR5::GFP grafted
pDR5::GFP cut
pDR5::GFP ungrafted
Fluorescence intensity
Days after grafting
F
pTCSn::GFP grafted
pTCSn::GFP ungrafted
Fluorescence intensity
Days after grafting
pTCSn::GFP-ER/self
G
1 DAG
scion
rootstock
6 DAG
10 DAG
pDR5::GFP-ER controls
H
ungrafted
I
I
J
5 DAC
cut shoot
K
K
L
5 DAC
cut root
pARR5::GFP controls
M
ungrafted
N
N
O
6 DAC
cut shoot
P
6 DAC
Q
cut root
Q
pTCSn::GFP-ER controls
R
ungrafted
S
S
T
6 DAC
cut shoot
U
6 DAC
V
cut root
V

Figure S4. Auxin and cytokinin response are spatially and temporally controlled during vasculature connection, related to Figure 4.

A-C) Plants expressing auxin or cytokinin response reporters were self-grafted, and 48 hours later, a drop of agar containing 1.2μM benzyl adenine (BA) dissolved in dimethyl sulfoxide (DMSO), 10μM 1-naphthaleneacetic acid (NAA) dissolved in DMSO, or DMSO was added to the hypocotyl. Graft junctions were imaged at 0 and 6 hours after hormone treatment, and fluorescence intensity calculated for grafted (n=5-6) and ungrafted individuals (n=6). Mean +/- SEM is shown. Ungrafted individuals did not show a substantial response to the hormone treatment, presumably due to the low permeability of the hormone.

D) Cytokinin response (*pARR5::GFP*) increases upon graft formation in self-grafted individuals (n=9), whereas ungrafted (n=4) and cut (n=3-4) individuals do not show a strong response. The same plants were imaged and quantified daily, and a representative individual is shown in Figure 4E. Mean +/- SEM is shown.

E) Auxin response (*pDR5rev::GFP-ER*) increases upon graft formation in self-grafted (n=8) and cut (n=4) individuals, whereas ungrafted individuals (n=4) do not show a strong response. The same plants were imaged and quantified daily, and a representative individual is shown in Figure 4A. Mean +/- SEM is shown.

F) Cytokinin response (*pTCSn::GFP-ER*) increases upon graft formation in self-grafted individuals (n=4), whereas ungrafted (n=7) individuals do not show a strong response. The same plants were imaged and quantified daily, and a representative individual is shown in Figure S4G. Mean +/- SEM is shown.

G) The cytokinin responsive *pTCSn::GFP-ER* gene increases expression at the graft junction during graft formation.

H-L) In longitudinal projections and transverse hand sections, the auxin responsive *pDR5rev::GFP-ER* gene has low expression levels in the vascular cambium and pericycle of the ungrafted hypocotyls (H,I). Cut but ungrafted *pDR5rev::GFP-ER* expresses strongly in the vascular tissue of the shoot hypocotyl, and weakly in the root hypocotyl (J-L).

M-Q) In longitudinal projections and transverse hand sections, the cytokinin-responsive *pARR5::GFP* gene shows weak expression in the phloem poles in ungrafted hypocotyls (M,N). Cut but ungrafted *pARR5::GFP* does not express in the shoot hypocotyl, but shows expression throughout the root hypocotyl (O-Q).

R-V) In longitudinal projections and transverse hand sections, the cytokinin-responsive *pTCSn::GFP-ER* gene shows weak expression in the phloem poles in ungrafted hypocotyls (R,S). Cut but ungrafted *pTCSn::GFP-ER* does not express in the shoot hypocotyl, but shows expression throughout the root hypocotyl (T-V).

G-V) Solid lines represent where transverse hand sections were made. Asterisks indicate pericycle cells, and arrows point to the orientation of the xylem. Scale bar is 25μm. Plants express *pUBQ10::PM-tdTomato* to outline cell membranes, except for panel K, O and P which are counterstained with FM4-64.

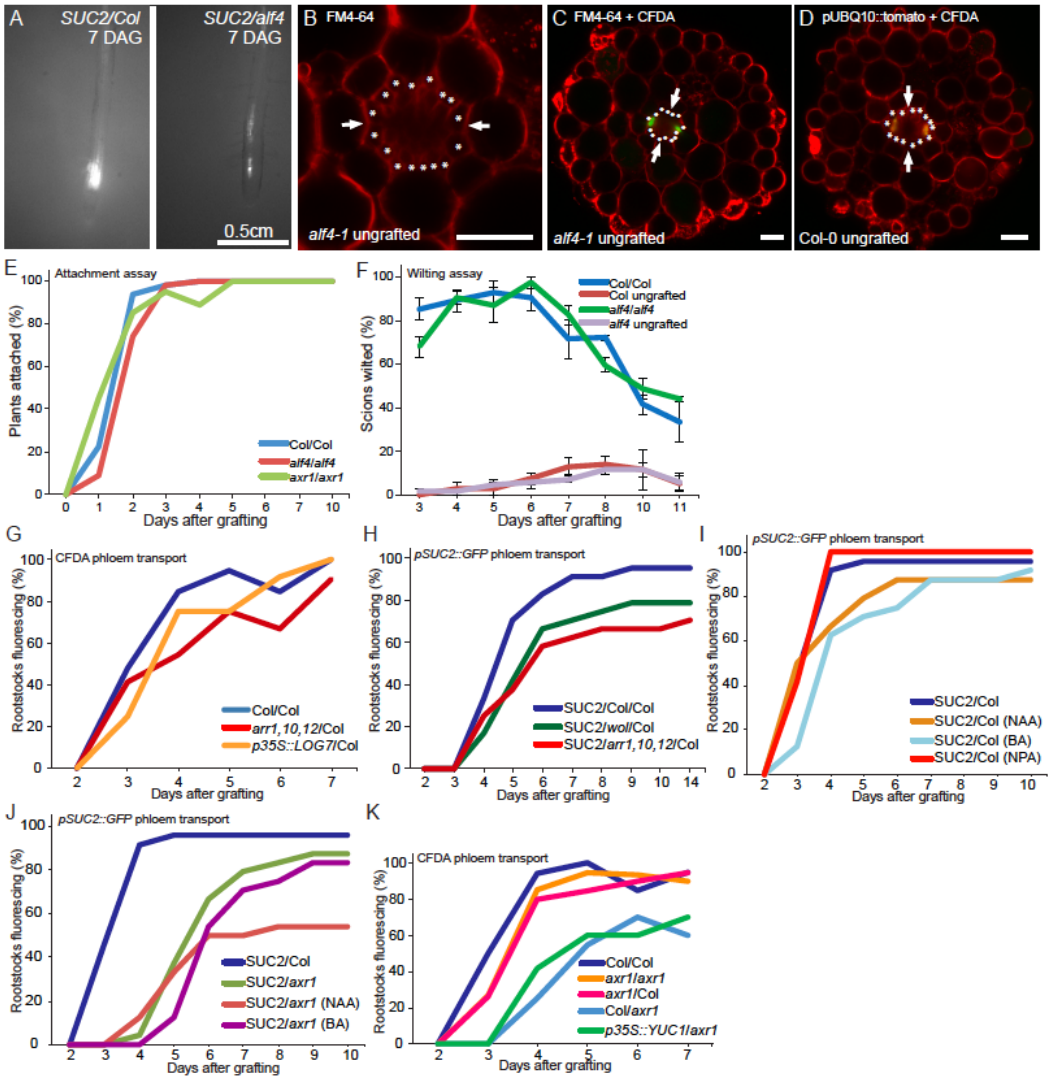

Figure S5. Modifying cytokinin response or auxin levels does not substantially affect phloem formation, related to Figure 5.

A) GFP intensity in grafted *pSUC2::GFP*/Col root tips is substantially stronger than GFP intensity in grafted *pSUC2::GFP*/*alf4-1* root tips seven DAG.

B-D) *alf4-1* appears to have normal vascular arrangement in 13 day-old hypocotyls (B), and contains two functional phloem poles similar to wild type plants, as tested by 1 hour CFDA application to the cotyledons and hand sectioning through the hypocotyl (C, D). Asterisks indicate pericycle cells, and arrows point to the orientation of the xylem. Scale bar is 25μm.

E) Self-grafted Col, *axr1-12* or *alf4-1* plants have similar rates of attachment. Mean shown from 20-96 plants per experiment and 1-3 experiments.

F) *alf4-1* does not affect rates of wilting in grafted individuals. Mean shown from 3 experiments with 15-25 plants per time point per experiment (+/- SEM).

G) Reducing cytokinin response (*arr1,10,12* mutant) or increasing cytokinin levels (*p35S::LOG7* transgenic line) in the scion does not affect phloem connection to the rootstock. Mean shown from 10-20 plants per time point per graft combination.

H) Reducing cytokinin response (*arr1,10,12* or *wol* mutant) in the hypocotyl reduces phloem reconnection by approximately one day. Mean shown from 24 plants per graft combination.

I-J) Grafting on exogenous NAA (0.5μM), BA (0.06μM) or 1-N-naphthylphthalamic acid (NPA) (5μM) did not substantially inhibit graft formation (I), and did not rescue *axr1-12* rootstocks (J). Mean shown from 24 plants per graft combination.

K) Grafting a scion with excess auxin (*p35S::YUC1* mutant) did not rescue the *axr1-12* rootstock. Mean shown from 15-20 plants per time point per graft combination.

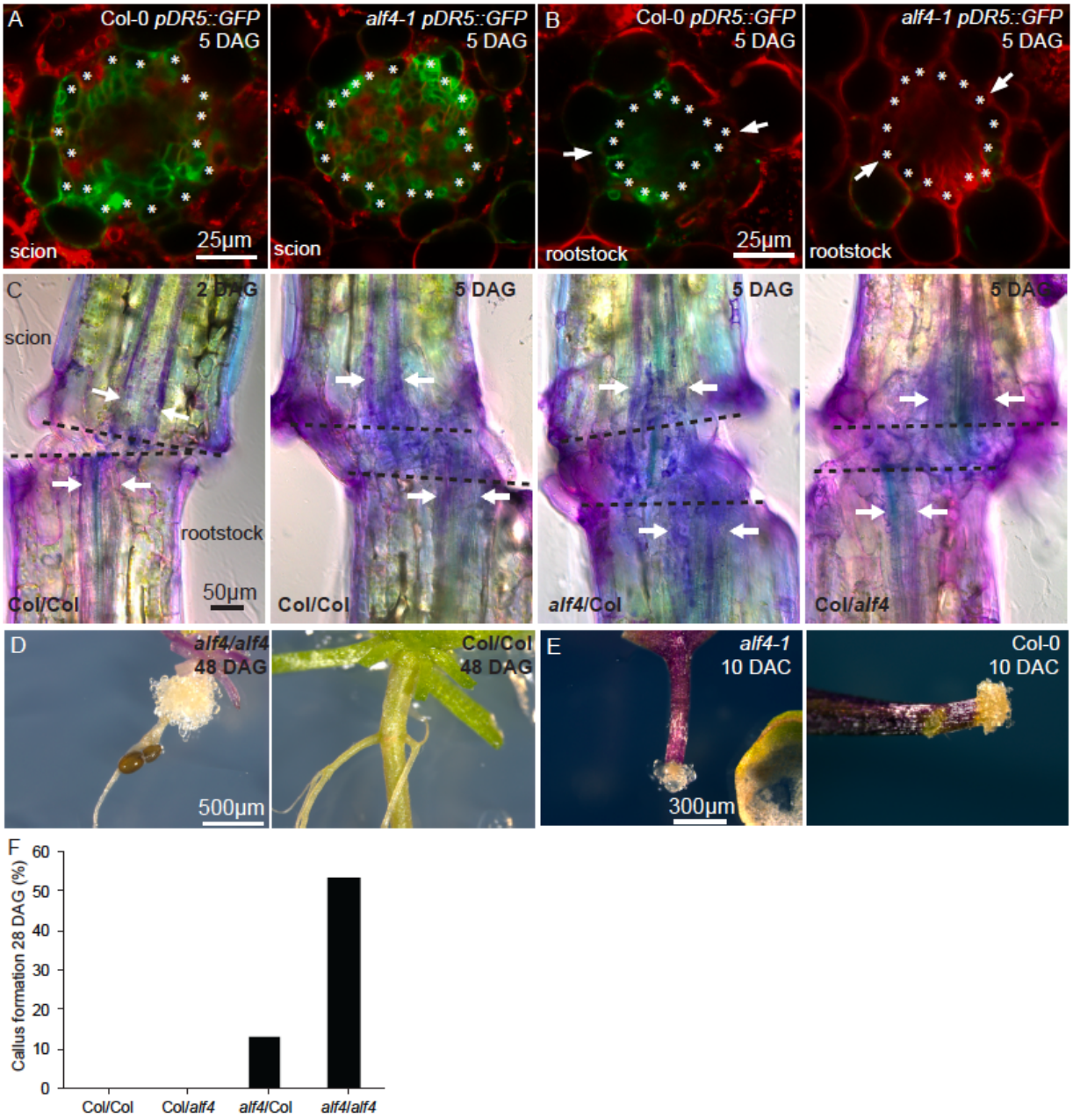

Figure S6. *alf4* is perturbed in auxin response, rootstock vascular growth and shows enhanced callus formation at the graft junction, related to Figure 6.
A-B) In transverse hand sections, *pDR5::GFP-ER* response is present 50µM above the graft junction in wild-type and *alf4-1* rootstocks (A). 50µM below the graft junction, auxin response is detected in the pericycle of wild-type plants, but not in *alf4-1* rootstocks (B). Asterisks indicate pericycle cells, and arrows point to the orientation of the xylem. Sections are counter stained with FM4-64.
C) In longitudinal hand sections, vascular cells (denoted by white arrows on either side) expand in the scion and rootstock upon graft formation in wild-type individuals, but not in an *alf4* rootstock at five DAG.
D-E) Wound-induced callus forms at the graft junction in *alf4*/*alf4* grafts, but not in Col/Col grafts (D). Wound-induced callus forms upon cutting both *alf4* and Col-0 leaf petioles (E).
F) Wound-induced callus formation requires an *alf4* scion, and is enhanced by an *alf4* rootstock. *alf4-1* and Col scions or rootstocks were used for grafting (scion/rootstock notation) and the presence or absence of callus at the graft junction was measured at 28 DAG. n=35-68 plants per graft combination were assayed.

Table S1. A list of genotypes used in this study.

	Pathway	Allele	Back ground	AGI accession number	Reference
Mutant	Auxin	*alf4-1*	Col	AT5G11030	[S1]
		alf4-063	Col	AT5G11030	[S2]
		arf2-8	Col	AT5G62000	[S3]
		arf6-2	Col	AT1G30330	[S4]
		arf8-3	Col	AT5G37020	[S4]
		arf8 p35S::ARF17	Col	AT5G37020; AT1G77850	[S5]
		arf7-1 arf19-1	Col	AT5G20730; AT1G19220	[S3]
		aux1-7	Col	AT2G38120	[S6]
		axr1-12	Col	AT1G05180	[S7]
		axr4-2	Col	AT1G54990	[S8]
		iaa1 (axr5-1)	Col	AT4G14560	[S9]
		iaa7 (axr2-1)	Col	AT3G23050	[S10]
		iaa12 (bdl-2)	Col	AT1G04550	[S11]
		iaa14 (slr1)	Col	AT4G14550	[S12]
		iaa17 (axr3-1)	Col	AT1G04250	[S13]
		iaa18 (crane-2)	Col	AT1G51950	[S14]
		iaa18-1	Ler	AT1G51950	[S15]
		iaa19 (msg2-1)	Col	AT3G15540	[S16]
		iaa28-1	Ws	AT5G25890	[S17]
		pin3-3 pin4-3	Col	AT1G70940; AT2G01420	[S18]
		pin4-3 pin7-1	Col	AT2G01420; AT1G23080	[S18]
		pin3-3 pin4-3 pin7-1	Col	AT1G70940; AT2G01420; AT1G23080	[S18]
		tir1-1	Col	AT3G62980	[S19]
		tir1-1 afb2-3	Col	AT3G62980; AT3G26810	[S20]
		tir1 afb2 afb3	Col	AT3G62980; AT3G26810	[S20]
		tir1 afb1 afb2/+ afb3	Col	AT3G62980; AT4G03190; AT3G26810; AT1G12820	[S20]
		tir3-101	Col	AT3G02260	[S21]
		p35S::YUC1	Col	AT4G32540	[S22]
		p35S::iaaL	Col		[S23]
		iaa3 (shy2-2)	Ler	AT1G04240	[S24]
		iaa3 (shy2-31)	Ler	AT1G04240	[S25]
	Cytokinin	*ahk2-2 ahk3-3*	Col	AT5G35750; AT1G27320	[S26]
		ahp6-3	Col	AT1G80100	[S27]
		amp1-1	Col	AT3G54720	[S28]
		arr1 arr12	Col	AT3G16857; AT2G25180	[S29]

	arr1 arr10 arr12	Col	AT3G16857; AT4G31920; AT2G25180	[S29]
	cre1-12 ahk3-3	Col	AT2G01830; AT1G27320	[S26]
	ipt1 ipt3 ipt5 ipt7	Col	AT1G68460; AT3G63110; AT5G19040; AT3G23630	[S30]
	ipt-161	C24		[S31]
	p35S::CKX1	Col	AT2G41510	[S32]
	p35S::CKX3	Col	AT5G56970	[S32]
	p35S::LOG7	Col	AT5G06300	[S33]
	wol	Col	AT2G01830	[S34]
Ethylene	*ctr1-1*	Col	AT5G03730	[S35]
	ein2-1	Col	AT5G03280	[S36]
	eto2	Col	AT5G65800	[S35]
	etr1-1	Col	AT1G66340	[S37]
Other	*scr-3*	Col	AT3G54220	[S38]
	shr-2	Col (*gl1*)	AT4G37650	[S38]
	*pWIND1::WIND1-*SRDX	Col		[S39]
	Capsella rubella	N/A		
	Cardamine hirsuta (Oxford)	N/A		[S40]
	Olimarabidopsis pumila	N/A		
	Thellungiella salsuginea (Shandong)	N/A		
Fluorescent Reporters	*pSUC2::GFP*	Col		[S41]
	pUBQ10::PM-tdTomato	Col		[S42]
	pWIND1::GFP	Col		[S39]
	p35S::YFP-ER	Col		[S43]
	p35S::GFP-ER	Col		[S43]
	pCASP1::NLS-GFP	Col		[S44]
	pTCSn::GFP-ER	Col		[S45]
	pDR5rev::GFP-ER	Col		[S46]
	pARR5::GFP	Ws		[S47]
	p35S::GFP-LTi p35S:: H2B-RFP	mixed		[S48]
	p35S::mCherry-LTi p35S::H2B-YFP	mixed		[S48]
	p35S::GFP	Col		[S49]

Supplemental Experimental Procedures

Plant Material

Arabidopsis thaliana wild type, accession Columbia was used throughout, unless otherwise indicated. All the lines used in this study have been previously published, and information on them is present in Table S1. *alf4-1* plants were from heterozygous or homozygous parents. Homozygous seeds were obtained by grafting a wild type rootstock to an *alf4-1* scion, and self-pollinating by hand. Progeny were verified by primers that identified the *alf4-1* deletion (5'-CGATGAATACTTAGCTGTTTCGTG-3' and 5'-TCCAAAGCTACGTTCTCATACAAA-3'). These plants were phenotypically indistinguishable from *alf4-1* mutants derived from a heterozygous parent.

Arabidopsis grafting

Ethanol sterilised *Arabidopsis* seeds were germinated on 1/2 Murashige and Skoog (MS) medium + 1% bacto agar (pH5.7; no sucrose) and grown on vertically-mounted Petri dishes under short day conditions (8 hours of 80-100μmoles light) at 20°C. Grafting was performed in a laminar flow hood with a portable dissecting microscope. 7 day-old seedlings were transferred to 9cm Petri dishes that contained one layer of 2.5x4cm sterilised Hybond N membrane (GE Healthcare) on top of two layers of 3mm Chr Whatman paper (8cm sterilised disks; Scientific Laboratory Supplies). The paper was kept moist using sterile distilled water. A transverse cut was made through the hypocotyl close to the shoot using a vascular dissecting knife (Ultra Fine Micro Knife; Fine Science Tools). In addition, one cotyledon was removed to assist in aligning the grafted pieces. In the case of self-grafts, an additional 1mm segment was cut from the hypocotyl and discarded. Grafts were assembled by butt alignment of the two cut halves with no supporting collar (butt end graft). After grafting, Petri dishes were sealed with parafilm, mounted vertically under short day conditions and monitored for 10 days at 20°C.

For grafting on a microscope coverslip, a 10cm square Petri dish was modified by removing a 2.5 x 4cm section of plastic from the back, and gluing a microscope coverslip

in its place (see Figure S1). The Petri dish was sterlised with ethanol and a 2.5x4 cm rectangle of Hybond N membrane was placed on top, just overlapping part of the microscope cover slip. Three 3 x 8cm strips of Whatman paper were placed at the sides and base of the Petri dish. The Whatman paper and Hybond N were moistened with sterile water. 7 days after germination, *Arabidopsis* seedlings were placed on the coverslip, so that the roots were on the Hybond N, and hypocotyls were on the coverslip. Grafting proceeded as above, and plates were sealed with Parafilm and graft junctions imaged through the coverslip with a 10X or 20X dry objective on a Zeiss 700 or 780 confocal microscope (see Figure S1).

Microscope sample preparation for cross-sections and whole mounts

Grafted hypocotyls were placed in a molten 3% agar solution, and left to solidify. A double-sided razor blade was used to cut through the hypocotyl to make transverse or longitudinal hand sections. Sections were placed on a glass coverslip, and 1% molten agar placed around the sample to glue it to the coverslip. For toluidine blue stained sections, a solution of 0.1% toluidine blue (Sigma Aldrich) was used to stain the sample. Water was then added immediately, and the sample imaged using a 20X water-dipping objective. For visualising xylem and Casparian strips, samples were cleared using a previously described protocol [S50] and mounted in 50% glycerol for visualisation with a Zeiss Axioimager.M2 microscope with DIC optics (xylem) or a Zeiss 780 confocal microscope with a 488 laser to detect autofluorescence from lignin [S51].

Microscope imaging and image analysis

Fluorescent images of whole-mount or hand-sectioned graft junctions were taken on a Zeiss LSM-700 or LSM-780 upright laser scanning confocal microscope fitted with a Zeiss W Plan-Apochromat 20X/1.0 DIC water-dipping objective or a Plan-Apochromat 20X/0.8 or Plan-Apochromat 10X/0.45 dry objective. GFP and YFP excitation was achieved with a 488nm argon laser (Zeiss 780) or 488nm solid-state laser (Zeiss 700) with the power set between 3-15%. FM4-64, RFP, mCherry and Tomato fluorescent

protein excitation was achieved with a 561nm solid-state laser with the power set between 0.3-12%. Bright-field transmitted light was obtained using a T-PMT detector. Fluorescent images of interstock grafts were taken on a Zeiss V12 dissecting microscope fitted with a Hamamatsu EM-CCD camera and GFP and YFP filters. A Zeiss V12 dissecting microscope was used to image carboxyfluorescein diacetate (CFDA) fluorescence, and GFP fluorescence from *pSUC2::GFP* scions to wild-type roots. Colour images were taken on a Zeiss V20 dissecting microscope. Images were processed using FIJI software. Brightness and image contrast were adjusted for controls and samples equally. Signal intensities of the bright-field transmitted light (T-PMT) and plasma membrane (FM4-64) channels were adjusted for some entire images to show tissue and cell boundaries where differences arose due to partial or excessive staining. For longitudinal projection images, z-stack projections are shown and made using the average intensity function with FIJI. For the *pDR5rev::GFP-ER* and *pTCSn::GFP-ER* *pUBQ10::PM-tdTomato* longitudinal images, z-stack projections were made from the stacks containing the vascular tissue. For the lignin longitudinal images, z-stack projections were made from the stacks containing the Casparian strip.

Hormone response assays

For hormone response assays, *Arabidopsis* plants were grafted on a coverslip (Figure S1). 1.2μM benzyl adenine (BA) or 10μM 1-naphthaleneacetic acid (NAA) were dissolved in 0.1% dimethyl sulfoxide (DMSO) and added to 1/2 MS + 1% bacto agar (pH5.7) and left to solidify. 48 hours after grafting, plates were opened and 2mm square blocks of agar containing BA, NAA or DMSO only (no hormone control) were placed next to the graft junction. Plates were sealed, and graft junctions were imaged at 0 and 6 hours after hormone treatment.

For phloem connectivity assays, *Arabidopsis* plants were germinated on 1/2 MS media and transferred to media containing hormones four days after germination, and three days before grafting. Plants were grafted on damp 3mm Chr Whatman filter paper

containing 0.06μM BA, 0.5μM NAA, 5μM 1-N-naphthylphthalamic acid (NPA) or DMSO, and left to recover for ten days on the hormone-containing Whatman paper.

Attachment assays

After grafting, *Arabidopsis* plants were picked up using forceps at the root/hypocotyl junction. If the scion remained attached during the manipulation, then the graft was considered attached.

Xylem assays

CFDA assays – CFDA (Cambridge Bioscience) was dissolved in DMSO (1mg per 10μl DMSO), and then 4.6μl added to 1ml of 1/2 MS + Gamborg's B5 vitamins (Duchefa Biochemie) + 0.8% bacto agar (pH 6.7) to make a final concentration of 1 mM. 500μl of solution was pipetted in a line into an empty 9cm Petri dish, and allowed to solidify. Grafted *Arabidopsis* or ungrafted controls had their roots cut off 2-3mm below the root/hypocotyl junction and the cut surface was placed in the solidified CFDA-agar solution. 20 minutes after placing the cut *Arabidopsis* plants in the CFDA-agar solution, fluorescence in the cotyledon vasculature was observed under a Zeiss V12 dissecting scope with a YFP filter and plants scored as either fluorescing or not. 20 minutes was chosen as a time point as it was the time that allowed the vast majority (>95%) of the ungrafted control plants to take up the dye, yet minimize the time which fluorescent dye might pass across the graft junction through methods other than through a continuous vascular connection, such as by apoplastic movement. It also reduced the influence of radial movement of CFDA from the vasculature.

Wilting assays - after imaging the above assay, the Petri dish was left at room temperature with the lid on (but no other form of sealing). Plants were then checked for wilting. Plants were scored as wilted if, after 24 hours of placing in the CFDA-agar solution, they showed strong collapsing of the cotyledon leaf surface. After CFDA

application and wilt scoring, grafts were discarded, and new plants used for the next time point.

Phloem assays

CFDA assays - CFDA was dissolved in DMSO (1mg per 10µl DMSO), and then 4.6µl added to 1ml of 1/2 MS + Gamborg's B5 vitamins + 0.8% bacto agar (pH 6.7) to make a final concentration of 1 mM. Cotyledons of grafted plants or ungrafted controls were lightly damaged by grasping the leaf with narrow forceps. A drop (~1µl) of CFDA solution was pipetted onto the macerated point while the agar was still liquid. After 1 hour, fluorescence in the root vasculature was observed under a Zeiss V12 dissecting microscope with a YFP filter and plants scored as either fluorescing or not. 1 hour was chosen as a time point as it was the time that allowed the vast majority (>95%) of the ungrafted control plants to take up the dye, yet minimize the time which fluorescent dye might pass across the graft junction through methods other than continuous vascular, such as apoplastic movement. It also reduced the influence of radial movement of CFDA from the vasculature. After CFDA application and scoring, grafts were discarded, and new plants used for the next time point.

pSUC2::GFP assays – *pSUC2::GFP* Col-0 scions were grafted to wild type or mutant roots, and roots were observed with a Zeiss V12 dissecting microscope 0 to 10 days after grafting (DAG) with a GFP filter. The number of plants with fluorescent roots was counted daily. The same plants were observed during the course of the 10-day assay.

H4 in situ hybridisation

In situ hybridisation with *HISTONE H4* RNA antisense probe was performed on seedlings two and three DAG in accordance with standard protocols [S52]. The quantification of the *HIS4* expression and the calculation of the mitotic index were done as described [S53] with the following modifications: All images were acquired using a Zeiss AxioCamMR3 camera with the Zeiss AxioVision Image software. Images for image analysis were

captured with a 20x lens in brightfield with fully opened diaphragm at 1388 x 1040 picture size. The threshold was determined by the mean intensity of unstained cell populations in the scion meristem region or young leaves of the same section minus four standard deviations. These tissues were chosen for background determination because they contained a continuous array of small cells, similar to the vascular region of graft junctions, in contrast to the surrounding large vacuolised cells of the hypocotyl. The mitotic index was determined as the ratio between the total number of thresholded pixels to a defined total number of 60.000 pixels, which represents the area of the vascular tissue of the graft analysed for the scion and rootstock. Up to 5 sections per graft showing the vasculature were analysed from 10-15 grafts per time point, and the mean intensity was calculated. The calculation of the mitotic index was done using the ImageJ software and Excel. Statistical analysis was performed in R. Data were tested for normality using a Shapiro-Wilk test and means were compared pairwise using Welch's t test.

Supplemental References

S1. Celenza, J.L., Jr., Grisafi, P.L., and Fink, G.R. (1995). A pathway for lateral root formation in Arabidopsis thaliana. Genes Dev *9*, 2131-2142.

S2. DiDonato, R.J., Arbuckle, E., Buker, S., Sheets, J., Tobar, J., Totong, R., Grisafi, P., Fink, G.R., and Celenza, J.L. (2004). Arabidopsis ALF4 encodes a nuclear-localized protein required for lateral root formation. The Plant journal *37*, 340-353.

S3. Okushima, Y., Overvoorde, P.J., Arima, K., Alonso, J.M., Chan, A., Chang, C., Ecker, J.R., Hughes, B., Lui, A., Nguyen, D., et al. (2005). Functional genomic analysis of the AUXIN RESPONSE FACTOR gene family members in Arabidopsis thaliana: unique and overlapping functions of ARF7 and ARF19. Plant Cell *17*, 444-463.

S4. Nagpal, P., Ellis, C.M., Weber, H., Ploense, S.E., Barkawi, L.S., Guilfoyle, T.J., Hagen, G., Alonso, J.M., Cohen, J.D., Farmer, E.E., et al. (2005). Auxin response factors ARF6 and ARF8 promote jasmonic acid production and flower maturation. Development *132*, 4107-4118.

S5. Gutierrez, L., Bussell, J.D., Pacurar, D.I., Schwambach, J., Pacurar, M., and Bellini, C. (2009). Phenotypic plasticity of adventitious rooting in Arabidopsis is controlled by complex regulation of AUXIN RESPONSE FACTOR transcripts and microRNA abundance. Plant Cell *21*, 3119-3132.

S6. Bennett, M.J., Marchant, A., Green, H.G., May, S.T., Ward, S.P., Millner, P.A., Walker, A.R., Schulz, B., and Feldmann, K.A. (1996). Arabidopsis AUX1 gene: a permease-like regulator of root gravitropism. Science *273*, 948-950.

S7. Lincoln, C., Britton, J.H., and Estelle, M. (1990). Growth and Development of the Axr1 Mutants of Arabidopsis. Plant Cell *2*, 1071-1080.

S8. Hobbie, L., and Estelle, M. (1995). The axr4 auxin-resistant mutants of Arabidopsis thaliana define a gene important for root gravitropism and lateral root initiation. The Plant journal *7*, 211-220.

S9. Yang, X., Lee, S., So, J.H., Dharmasiri, S., Dharmasiri, N., Ge, L., Jensen, C., Hangarter, R., Hobbie, L., and Estelle, M. (2004). The IAA1 protein is encoded by AXR5 and is a substrate of SCF(TIR1). The Plant journal *40*, 772-782.
S10. Wilson, A.K., Pickett, F.B., Turner, J.C., and Estelle, M. (1990). A dominant mutation in Arabidopsis confers resistance to auxin, ethylene and abscisic acid. Molecular & general genetics *222*, 377-383.
S11. Hayward, A., Stirnberg, P., Beveridge, C., and Leyser, O. (2009). Interactions between auxin and strigolactone in shoot branching control. Plant Physiol *151*, 400-412.
S12. Fukaki, H., Tameda, S., Masuda, H., and Tasaka, M. (2002). Lateral root formation is blocked by a gain-of-function mutation in the SOLITARY-ROOT/IAA14 gene of Arabidopsis. The Plant journal *29*, 153-168.
S13. Leyser, H.M., Pickett, F.B., Dharmasiri, S., and Estelle, M. (1996). Mutations in the AXR3 gene of Arabidopsis result in altered auxin response including ectopic expression from the SAUR-AC1 promoter. The Plant journal *10*, 403-413.
S14. Uehara, T., Okushima, Y., Mimura, T., Tasaka, M., and Fukaki, H. (2008). Domain II mutations in CRANE/IAA18 suppress lateral root formation and affect shoot development in Arabidopsis thaliana. Plant Cell Physiol *49*, 1025-1038.
S15. Ploense, S.E., Wu, M.F., Nagpal, P., and Reed, J.W. (2009). A gain-of-function mutation in IAA18 alters Arabidopsis embryonic apical patterning. Development *136*, 1509-1517.
S16. Tatematsu, K., Kumagai, S., Muto, H., Sato, A., Watahiki, M.K., Harper, R.M., Liscum, E., and Yamamoto, K.T. (2004). MASSUGU2 encodes Aux/IAA19, an auxin-regulated protein that functions together with the transcriptional activator NPH4/ARF7 to regulate differential growth responses of hypocotyl and formation of lateral roots in Arabidopsis thaliana. Plant Cell *16*, 379-393.
S17. Rogg, L.E., Lasswell, J., and Bartel, B. (2001). A gain-of-function mutation in IAA28 suppresses lateral root development. Plant Cell *13*, 465-480.
S18. Blilou, I., Xu, J., Wildwater, M., Willemsen, V., Paponov, I., Friml, J., Heidstra, R., Aida, M., Palme, K., and Scheres, B. (2005). The PIN auxin efflux facilitator network controls growth and patterning in Arabidopsis roots. Nature *433*, 39-44.
S19. Ruegger, M., Dewey, E., Gray, W.M., Hobbie, L., Turner, J., and Estelle, M. (1998). The TIR1 protein of Arabidopsis functions in auxin response and is related to human SKP2 and yeast grr1p. Genes Dev *12*, 198-207.
S20. Parry, G., Calderon-Villalobos, L.I., Prigge, M., Peret, B., Dharmasiri, S., Itoh, H., Lechner, E., Gray, W.M., Bennett, M., and Estelle, M. (2009). Complex regulation of the TIR1/AFB family of auxin receptors. P Natl Acad Sci USA *106*, 22540-22545.
S21. Bennett, T., Sieberer, T., Willett, B., Booker, J., Luschnig, C., and Leyser, O. (2006). The Arabidopsis MAX pathway controls shoot branching by regulating auxin transport. Curr Biol *16*, 553-563.
S22. Weigel, D., Ahn, J.H., Blazquez, M.A., Borevitz, J.O., Christensen, S.K., Fankhauser, C., Ferrandiz, C., Kardailsky, I., Malancharuvil, E.J., Neff, M.M., et al. (2000). Activation tagging in Arabidopsis. Plant Physiol *122*, 1003-1013.
S23. Jensen, P.J., Hangarter, R.P., and Estelle, M. (1998). Auxin transport is required for hypocotyl elongation in light-grown but not dark-grown Arabidopsis. Plant Physiol *116*, 455-462.
S24. Reed, J.W., Elumalai, R.P., and Chory, J. (1998). Suppressors of an Arabidopsis thaliana phyB mutation identify genes that control light signaling and hypocotyl elongation. Genetics *148*, 1295-1310.
S25. Knox, K., Grierson, C.S., and Leyser, O. (2003). AXR3 and SHY2 interact to regulate root hair development. Development *130*, 5769-5777.
S26. Higuchi, M., Pischke, M.S., Mahonen, A.P., Miyawaki, K., Hashimoto, Y., Seki, M., Kobayashi, M., Shinozaki, K., Kato, T., Tabata, S., et al. (2004). In planta functions of the Arabidopsis cytokinin receptor family. P Natl Acad Sci USA *101*, 8821-8826.

S27. Mahonen, A.P., Bishopp, A., Higuchi, M., Nieminen, K.M., Kinoshita, K., Tormakangas, K., Ikeda, Y., Oka, A., Kakimoto, T., and Helariutta, Y. (2006). Cytokinin signaling and its inhibitor AHP6 regulate cell fate during vascular development. Science *311*, 94-98.
S28. Chaudhury, A.M., Letham, S., Craig, S., and Dennis, E.S. (1993). amp1 - a mutant with high cytokinin levels and altered embryonic pattern, faster vegetative growth, constitutive photomorphogenesis and precocious flowering. The Plant Journal *4*, 907-916.
S29. Mason, M.G., Mathews, D.E., Argyros, D.A., Maxwell, B.B., Kieber, J.J., Alonso, J.M., Ecker, J.R., and Schaller, G.E. (2005). Multiple type-B response regulators mediate cytokinin signal transduction in Arabidopsis. Plant Cell *17*, 3007-3018.
S30. Miyawaki, K., Tarkowski, P., Matsumoto-Kitano, M., Kato, T., Sato, S., Tarkowska, D., Tabata, S., Sandberg, G., and Kakimoto, T. (2006). Roles of Arabidopsis ATP/ADP isopentenyltransferases and tRNA isopentenyltransferases in cytokinin biosynthesis. P Natl Acad Sci USA *103*, 16598-16603.
S31. van der Graff, E.E., Auer, C.A., and Hooykaas, P.J.J. (2001). Altered development of *Arabidopsis thaliana* carrying the *Agrobacterium tumefaciens* ipt gene is partially due to ethylene effects. Plant Growth Regulation *34*, 305-315.
S32. Werner, T., Motyka, V., Laucou, V., Smets, R., Van Onckelen, H., and Schmulling, T. (2003). Cytokinin-deficient transgenic Arabidopsis plants show multiple developmental alterations indicating opposite functions of cytokinins in the regulation of shoot and root meristem activity. Plant Cell *15*, 2532-2550.
S33. Kuroha, T., Tokunaga, H., Kojima, M., Ueda, N., Ishida, T., Nagawa, S., Fukuda, H., Sugimoto, K., and Sakakibara, H. (2009). Functional analyses of LONELY GUY cytokinin-activating enzymes reveal the importance of the direct activation pathway in Arabidopsis. Plant Cell *21*, 3152-3169.
S34. Mahonen, A.P., Bonke, M., Kauppinen, L., Riikonen, M., Benfey, P.N., and Helariutta, Y. (2000). A novel two-component hybrid molecule regulates vascular morphogenesis of the Arabidopsis root. Genes Dev *14*, 2938-2943.
S35. Kieber, J.J., Rothenberg, M., Roman, G., Feldmann, K.A., and Ecker, J.R. (1993). CTR1, a negative regulator of the ethylene response pathway in Arabidopsis, encodes a member of the raf family of protein kinases. Cell *72*, 427-441.
S36. Guzman, P., and Ecker, J.R. (1990). Exploiting the triple response of Arabidopsis to identify ethylene-related mutants. Plant Cell *2*, 513-523.
S37. Chang, C., Kwok, S.F., Bleecker, A.B., and Meyerowitz, E.M. (1993). Arabidopsis ethylene-response gene ETR1: similarity of product to two-component regulators. Science *262*, 539-544.
S38. Fukaki, H., Wysocka-Diller, J., Kato, T., Fujisawa, H., Benfey, P.N., and Tasaka, M. (1998). Genetic evidence that the endodermis is essential for shoot gravitropism in Arabidopsis thaliana. The Plant journal *14*, 425-430.
S39. Iwase, A., Mitsuda, N., Koyama, T., Hiratsu, K., Kojima, M., Arai, T., Inoue, Y., Seki, M., Sakakibara, H., Sugimoto, K., et al. (2011). The AP2/ERF Transcription Factor WIND1 Controls Cell Dedifferentiation in Arabidopsis. Curr Biol *21*, 508-514.
S40. Hay, A., and Tsiantis, M. (2006). The genetic basis for differences in leaf form between Arabidopsis thaliana and its wild relative Cardamine hirsuta. Nat Genet *38*, 942-947.
S41. Imlau, A., Truernit, E., and Sauer, N. (1999). Cell-to-cell and long-distance trafficking of the green fluorescent protein in the phloem and symplastic unloading of the protein into sink tissues. Plant Cell *11*, 309-322.
S42. Segonzac, C., Nimchuk, Z.L., Beck, M., Tarr, P.T., Robatzek, S., Meyerowitz, E.M., and Zipfel, C. (2012). The shoot apical meristem regulatory peptide CLV3 does not activate innate immunity. Plant Cell *24*, 3186-3192.
S43. Nelson, B.K., Cai, X., and Nebenfuhr, A. (2007). A multicolored set of in vivo organelle markers for co-localization studies in Arabidopsis and other plants. The Plant journal *51*, 1126-1136.

S44. Roppolo, D., De Rybel, B., Tendon, V.D., Pfister, A., Alassimone, J., Vermeer, J.E., Yamazaki, M., Stierhof, Y.D., Beeckman, T., and Geldner, N. (2011). A novel protein family mediates Casparian strip formation in the endodermis. Nature *473*, 380-383.
S45. Zurcher, E., Tavor-Deslex, D., Lituiev, D., Enkerli, K., Tarr, P.T., and Muller, B. (2013). A Robust and Sensitive Synthetic Sensor to Monitor the Transcriptional Output of the Cytokinin Signaling Network in Planta. Plant Physiol *161*, 1066-1075.
S46. Friml, J., Vieten, A., Sauer, M., Weijers, D., Schwarz, H., Hamann, T., Offringa, R., and Jurgens, G. (2003). Efflux-dependent auxin gradients establish the apical-basal axis of Arabidopsis. Nature *426*, 147-153.
S47. Yanai, O., Shani, E., Dolezal, K., Tarkowski, P., Sablowski, R., Sandberg, G., Samach, A., and Ori, N. (2005). Arabidopsis KNOXI proteins activate cytokinin biosynthesis. Curr Biol *15*, 1566-1571.
S48. Federici, F., Dupuy, L., Laplaze, L., Heisler, M., and Haseloff, J. (2012). Integrated genetic and computation methods for in planta cytometry. Nat Methods *9*, 483-485.
S49. Brosnan, C.A., Mitter, N., Christie, M., Smith, N.A., Waterhouse, P.M., and Carroll, B.J. (2007). Nuclear gene silencing directs reception of long-distance mRNA silencing in Arabidopsis. P Natl Acad Sci USA *104*, 14741-14746.
S50. Malamy, J.E., and Benfey, P.N. (1997). Organization and cell differentiation in lateral roots of Arabidopsis thaliana. Development *124*, 33-44.
S51. Lee, Y., Rubio, M.C., Alassimone, J., and Geldner, N. (2013). A mechanism for localized lignin deposition in the endodermis. Cell *153*, 402-412.
S52. Maier, A.T., Stehling-Sun, S., Wollmann, H., Demar, M., Hong, R.L., Haubeiss, S., Weigel, D., and Lohmann, J.U. (2009). Dual roles of the bZIP transcription factor PERIANTHIA in the control of floral architecture and homeotic gene expression. Development *136*, 1613-1620.
S53. Geier, F., Lohmann, J.U., Gerstung, M., Maier, A.T., Timmer, J., and Fleck, C. (2008). A quantitative and dynamic model for plant stem cell regulation. PLoS One *3*, e3553.